

1 Simulation of tree ring-widths with a model for primary production, carbon allocation
2 and growth

3 G. Li¹, S. P. Harrison^{1,2}, I. C. Prentice^{1,3}, D. Falster¹

4 ¹ Department of Biological Sciences, Macquarie University, North Ryde, NSW 2109, Australia.

5 ² School of Archaeology, Geography and Environmental Sciences (SAGES), Reading University, Reading,
6 United Kingdom.

7 ³ AXA Chair of Biosphere and Climate Impacts, Grand Challenges in Ecosystem and the Environment,
8 Department of Life Sciences and Grantham Institute for Climate Change, Imperial College London, Ascot,
9 United Kingdom.

10 Correspondence to: G. Li (guangqi.li@students.mq.edu.au)

11 Abstract

12 We present a simple, generic model of annual tree growth, called ‘T’. This model accepts input from a first-
13 principles light-use efficiency model (the P model). The P model provides values for Gross Primary
14 Production (GPP) per unit of absorbed photosynthetically active radiation (PAR). Absorbed PAR is estimated
15 from the current leaf area. GPP is allocated to foliage, transport-tissue, and fine root production and
16 respiration, in such a way as to satisfy well-understood dimensional and functional relationships. Our
17 approach thereby integrates two modelling approaches separately developed in the global carbon-cycle and
18 forest-science literature. The T model can represent both ontogenetic effects (impact of ageing) and the
19 effects of environmental variations and trends (climate and CO₂) on growth. Driven by local climate records,
20 the model was applied to simulate ring widths during 1958~2006 for multiple trees of *Pinus koraiensis* from
21 the Changbai Mountain, northeastern China. Each tree was initialised at its actual diameter at the time when
22 local climate records started. The model produces realistic simulations of the interannual variability in ring
23 width for different age cohorts (young, mature, old). Both the simulations and observations show a significant
24 positive response of tree-ring width to growing-season total photosynthetically active radiation (PAR₀) and
25 the ratio of actual to potential evapotranspiration (α), and a significant negative response to mean annual
26 temperature (MAT). The slopes of the simulated and observed relationships with PAR₀ and α are similar; the
27 negative response to MAT is underestimated by the model. Comparison of simulations with fixed and
28 changing atmospheric CO₂ concentration shows that CO₂ fertilization over the past 50 years is too small to be
29 distinguished in the ring-width data given ontogenetic trends and interannual variability in climate.

31 Forests cover about 30% of the land surface (Bonan, 2008) and are estimated to contain 861 ± 66 PgC (Pan et
32 al., 2011). Inventory-based estimates show that forests have been a persistent carbon sink in recent decades,
33 with a gross uptake of 4.0 ± 0.5 PgCyear⁻¹ and a net uptake of 1.1 ± 0.8 PgCyear⁻¹ between 1990 and 2007 (Pan
34 et al., 2011). This is a significant amount in comparison with the amounts of carbon released from fossil fuel
35 burning, cement production and deforestation (9.5 ± 0.8 PgCyear⁻¹ in 2011: Ciais et al., 2013) and thus, forest
36 growth has a substantial effect on atmospheric CO₂ concentration and climate (Shevliakova et al., 2013).
37 However, there is considerable geographic variability in the trends in the carbon sink as well as the factors
38 controlling regional trends, and uncertainty about how forest growth and carbon sequestration will be affected
39 by climate change, and climate-driven changes in wildfire (Ciais et al., 2013; Moritz et al., 2013). The
40 changing importance of disturbance, and its influence on forest age, is likely to have a significant impact on
41 the ability of forests to act as carbon sinks. It is generally assumed that stand-level productivity stabilizes or
42 declines with age (Ryan et al., 1997; Caspersen et al., 2011). However, recent analyses have shown that mass
43 growth rate (and hence carbon accumulation) by individual trees increases continuously with tree size
44 (Stephenson et al., 2014), pointing to a need to understand the relationship between individual and stand
45 growth rates. Predictions of future changes in the terrestrial carbon cycle (e.g. Friedlingstein and Prentice,
46 2010) rely on ecosystem models that explicitly represent leaf-level processes such as photosynthesis, but in
47 most cases do not incorporate the response of individual trees. In models that do consider individual tree
48 growth (e.g. ED: Moorcroft et al 2001, Medvigy et al. 2012; LPJ-GUESS: Smith et al., 2001; Claesson and
49 Nycander, 2013), little attention has been paid to evaluating the realism of simulated radial growth.
50 Incorporating the response of individual trees to climate and environmental change within such modelling
51 frameworks should help to provide more realistic estimates of the role of forests in the global carbon cycle.

52 Climate factors, such as temperature and moisture availability during the growing season, are important
53 drivers of tree growth (Harrison et al., 2010). This forms the basis for reconstructing historical climate
54 changes from tree-ring records of annual growth (Fritts, 2012). However, photosynthetically active radiation
55 (PAR) is the principal driver of photosynthesis. Models for primary production that use temperature, not PAR,
56 implicitly rely on the far-from-perfect correlation between temperature and PAR (Wang et al., 2014). PAR
57 can change independently from temperature (through changes in cloudiness affecting PAR or atmospheric
58 circulation changes affecting temperature) and this may help to explain why statistical relationships between
59 tree growth and temperature at some high latitude and high elevation sites appear to breakdown in recent
60 decades (D'Arrigo et al., 2008). CO₂ concentration also has an impact on tree growth, although its magnitude
61 is still controversial: trends in tree growth have been attributed to increasing atmospheric CO₂ concentration
62 in some studies (Wullschleger et al., 2002; Körner, 2006; Huang et al., 2007; Koutavas, 2013) and not others
63 (Miller, 1986; Luo et al., 2004; Reich et al., 2006). To resolve these apparent conflicts, and to understand tree
64 growth processes better, it is necessary to analyse the response of tree growth to multiple factors acting
65 simultaneously, including solar radiation, climate, CO₂, and ontogenetic stage.

66 Modelling is needed for this purpose. Empirical models of annual tree growth and climate variables
67 (temperature and precipitation) have been used to simulate tree radial growth (Fritts, 2012). Process-based
68 bioclimatic models might be preferable, however, because this allows other factors to be taken into account
69 (e.g. the direct impact of CO₂ concentration on photosynthesis) and for non-stationarity in the response to
70 specific climate variables. Vaganov et al. (2006) and Rathgeber et al. (2005) have used bioclimatic variables
71 (temperature, and soil moisture availability) chosen to reflect physiological processes to simulate radial tree
72 growth. The MAIDEN model (Misson, 2004; Misson et al., 2004; see also MAIDENiso: Danis et al., 2012)
73 models the phenological and meteorological controls on NPP and explicitly allocates carbon to different
74 carbon pools (including the stem) on a daily basis using phenological stage-dependent rules. Nevertheless,
75 MAIDEN still requires tuning of several parameters.

76 Simple equations representing functional and geometric relationships can describe carbon allocation by trees
77 and make it possible to model individual tree growth (Yokozawa and Hara, 1995; Givnish, 1988; Falster et al.,
78 2011; King, 2011). Such models are built on measurable relationships, such as that between stem diameter
79 and height (Thomas, 1996; Ishii et al., 2000; Falster and Westoby, 2005), and crown area and diameter or
80 height (Duursma et al., 2010) that arise because of functional constraints on growth. The pipe model
81 represents the relationship between sapwood area and leaf area (Shinozaki et al., 1964; Yokozawa and Hara,
82 1995; Mäkelä et al., 2000). The ratio of fine root mass to foliage area provides the linkage between above and
83 below ground tissues (Falster et al., 2011). These functional relationships are expected to be stable through
84 ontogeny, which implies that the fraction of new carbon allocated to different compartments is variable
85 (Lloyd, 1999). In this paper, we combine the two modelling approaches previously developed in the global
86 carbon-cycle (ecophysiology) and forest-science (geometric and carbon allocation) literature to simulate
87 individual tree growth.

88

89 2 Methods

90 2.1 Model structure and derivation

91 We use a light-use efficiency model (the P model: Wang et al., 2014), driven by growing-season PAR, climate
92 and ambient CO₂ concentration inputs, to simulate gross primary production (GPP). The simulated GPP is
93 used as input to a species-based carbon allocation and functional geometric tree growth model (the T model)
94 to simulate individual tree growth (Fig. 1).

95 2.1.1 The P model

96 The P model is a simple but powerful light-use efficiency and photosynthesis model, which simulates GPP per
97 unit of absorbed PAR from latitude, elevation, temperature, precipitation and fractional cloud cover (Wang et
98 al., 2014). The climate observations used here are monthly temperature, precipitation and fractional cloud

99 cover, which are interpolated to a daily time step for subsequent calculations of the variables that determine
100 annual GPP.

101 Potential annual *GPP* is the product of the PAR incident on vegetation canopies (PAR_0), with the maximum
102 quantum efficiency of photosynthesis (Φ_0), the fraction of absorbed PAR ($fAPAR$), and the effect of
103 photorespiration and substrate limitation at subsaturating $[CO_2]$ represented as a function of the leaf-internal
104 $[CO_2]$ (c_i) and the photorespiratory compensation point (Γ^*), as shown in Eq. (1).

$$105 \quad GPP = \Phi_0 (PAR_0 \times fAPAR) (c_i - \Gamma^*) / (c_i + 2\Gamma^*) \quad (1)$$

106 where Φ_0 is set to 0.48 g C/ mol photon, based on a quantum efficiency of 0.05 mol C/ mol photon and a leaf
107 absorptance of 0.8. Daily PAR at the top of the atmosphere is calculated based on solar geometry and is
108 subsequently modified by transmission through the atmosphere, which is dependent on elevation and cloud
109 cover. Annual effective PAR (PAR_0) is calculated as the annual sum of daily PAR but taking into account the
110 low-temperature inhibition of photosynthesis and growth, using a linear ramp function to downweight PAR on
111 days with temperatures below 10 °C. Days with temperatures below 0°C do not contribute to PAR_0 . See
112 Wang et al. (2014) for details. In this application, we first calculated potential *GPP* with $fAPAR$ set to 1.
113 $fAPAR$ is not an input to the model but is calculated implicitly, from the foliage cover simulated by the T
114 model.

115 Leaf-internal $[CO_2]$ is obtained from the ambient $[CO_2]$ via the ‘least-cost hypothesis’ (Wright et al., 2003;
116 Prentice et al., 2014). Wang et al. (2014) provide a continuous prediction of the c_i/c_a ratio as a function of
117 environmental aridity, temperature and elevation based on this hypothesis:

$$118 \quad c_i/c_a = 1 / (1 + C \sqrt{(\eta \sqrt{D}) / K}) \quad (2)$$

119 where D is the cumulative water deficit over a year (proportional to an annual “effective value” of the vapour
120 pressure deficit: VPD), η is the dynamic viscosity of water, K is the effective Michaelis-Menten coefficient for
121 Rubisco-limited photosynthesis, and C is a constant. The difference between the annual actual and equilibrium
122 evapotranspiration is used as a proxy for D (see Prentice et al., 2013). D is calculated using the daily
123 interpolated temperature, precipitation and cloudiness data. Annual actual evapotranspiration is derived from
124 equilibrium evapotranspiration and precipitation using a simple soil moisture accounting scheme with a daily
125 time step, as described in Gallego-Sala et al. (2010). The temperature dependences of η and K follow Prentice
126 et al. (2014). Both K and η change steeply with temperature: K changes from 196 ppm at 10 °C to 1094 ppm
127 at 30 °C ; η decreases from 1.31 mPa s at 10 °C to only 0.798 mPa s at 30 °C.

128 The temperature dependence of Γ^* is described by an exponential closely approximating an Arrhenius
129 function (Bernacchi et al., 2003):

$$130 \quad \Gamma^* = \Gamma_{25}^* \exp(0.0512\Delta T) \quad (3)$$

131 where Γ_{25}^* is the value of Γ^* at 25 °C (4.331 Pa), and ΔT is the monthly temperature difference from 25 °C.

132 The P model has been shown to simulate well many of the global patterns of annual and maximum monthly
133 terrestrial GPP) by C₃ plants. The simulated seasonal cycle of GPP at different latitudes is supported by
134 analyses of CO₂ flux measurements (Wang et al., 2014).

135 2.1.2 The T model

136 We assume that potential GPP is the first-order driver of tree growth both at stand and individual level. The T
137 model translates potential GPP as simulated by the P model into individual tree growth, which depends on
138 foliage cover within the canopy and the respiration of non-green tissues, carbon allocation to different tissues,
139 and relationships between different dimensions of the tree. Although these relationships are often loosely
140 called “allometries”, true allometries (power functions) have the undesirable mathematical property for
141 growth modelling that, if the power is greater than one, the derivative evaluated at the start of growth is zero;
142 if the power is between zero and one, the derivative is infinite. We have therefore avoided the use of power
143 functions, except for geometric relationships where they are unambiguously correct.

144 *Functional geometric relationship*

146 Carbon is allocated to different tissues within the constraint of the basic functional or geometric relationships
147 between different dimensions of the tree.

148 Asymptotic height-diameter trajectories (Thomas, 1996; Ishii et al., 2000; Falster and Westoby, 2005) are
149 modeled as:

$$150 \quad H = H_m [1 - \exp(-aD/H_m)] \quad (4)$$

151 where H is the tree height, D is the basal diameter, H_m is the (asymptotic) maximum height, and a is the initial
152 slope of the relationship between height and diameter.

153 The model also requires the derivative of this relationship:

$$154 \quad dH/dD = a \exp(-aD/H_m) = a (1 - H/H_m). \quad (5)$$

155 The form of the stem is assumed to be paraboloid (Jonson, 1910; Larsen, 1963). It can be shown (assuming
156 the pipe model) that this form is uniquely consistent with a uniform vertical distribution of foliage area during
157 early growth, i.e. in the absence of heartwood. Here, the total stem mass (W_s) is expressed as a function of D
158 and H :

$$159 \quad W_s = (\pi/8) \rho_s D^2 H \quad (6)$$

160 where ρ_s is the density of the wood, and $(\pi/8) D^2 H$ is the volume of a paraboloid stem.

161 The relationship of diameter increment to stem increment is then given by:

162 $dW_s/dt = (\pi/8) \rho_s [D^2 (dH/dD) + 2 DH] dD/dt$ (7)

163 The projected crown area (A_c) is estimated from D and H using an empirical relationship:

164 $A_c = (\pi c/4a) DH$ (8)

165 where c is the initial ratio of crown area to stem cross-sectional area. This relationship was chosen as an
 166 intermediate between previously published expressions that relate A_c either to D^2 or H . It is consistent with
 167 reported allometric coefficients typically between 1 and 2 for the relationship between A_c and D .

168 Crown fraction (f_c) is also derived from H and D . As we assumed the stem to be paraboloid, the stem cross
 169 sectional area at height z is :

170 $A_s(z) = A_s (1-z/H)$ (9)

171 where A_s is the basal area: $A_s = (\pi/4)D^2$. We find the height (z^*) at which the ratio of foliage area (A_f) to stem
 172 area at height z^* ($A_s(z^*)$) is the same as the initial ratio of crown area to stem cross-sectional area (c). We
 173 obtain crown area (A_c) from:

174 $A_c = c A_s(z^*) = c A_s (1-z^*/H)$. (10)

175 Combining this with Eq. (8), we obtain $(\pi c/4a) DH = c A_s (1-z^*/H)$, which reduces to:

176 $f_c = (1-z^*/H) = H/aD$. (11)

177 The initial slope (a) is in principle dependent both on species growth form and on ambient conditions,
 178 including light availability. Here it is determined directly from observations.

179 *Carbon allocation*

180 Actual GPP (P) is obtained from potential GPP (P_0) using Beer's law (Jarvis and Leverenz, 1983):

181 $P = P_0 A_c (1 - \exp(-kL))$ (12)

182 where k is the extinction coefficient for PAR, and L is the leaf area index within the crown.

183 Net primary production (NPP) is derived from annual GPP, corrected for foliage respiration (which is set at
 184 10% of total GPP, an approximation based on the theory developed by Prentice et al., 2014 and Wang et al.,
 185 2014), by further deducting growth respiration and the maintenance respiration of sapwood and fine roots.
 186 Growth respiration is assumed to be proportional to NPP, following:

187 $P_{net} = y(P - R_m) = y (P - W_s r_s - \zeta \sigma W_f r_f)$ (13)

188 where P_{net} is NPP, R_m is the maintenance respiration of stem and fine roots, and y is the 'yield factor'
 189 accounting for growth respiration. Total maintenance respiration of non-green parts comprises fine-root

190 respiration ($\zeta \sigma W_f r_r$, where ζ is the ratio of fine-root mass to foliage area, σ is the specific leaf area, W_f is the
 191 mass of carbon in foliage ($(1/\sigma) L A_c$), and r_r is the specific respiration rate of fine roots), and stem (sapwood)
 192 respiration ($W_s r_s$, where W_s is the mass of carbon in sapwood, and r_s is the specific respiration rate of
 193 sapwood). W_s can be estimated from A_c through the pipe model:

$$194 \quad W_s = L A_c v_H \rho_s H_f \quad (14)$$

195 where v_H is the Huber value (ratio of sapwood to leaf area; Cruiziat et al., 2002), and H_f is the mean foliage
 196 height $H (1 - f_c/2)$. The constraint that the initial sapwood area must be equal to the stem cross-sectional area
 197 leads to the following identity: $L c v_H = 1$.

198 NPP is allocated to stem increment (dW_s/dt), foliage increment (dW_f/dt), fine-root increment ($\zeta \sigma dW_f/dt$),
 199 foliage turnover (W_f/τ_f , where τ_f is the turnover time of foliage), and fine-root turnover ($\zeta \sigma W_f/\tau_r$, where τ_r is
 200 the turnover time of fine roots). For simplicity, in common with many models, we do not consider allocation
 201 to branches and coarse roots separately from allocation to stem:

$$202 \quad P_{net} = dW_s/dt + (1 + \zeta \sigma) dW_f/dt + (1/\tau_f + \zeta \sigma/\tau_r) W_f \quad (15)$$

203 From Eq. (13) and Eq. (15), the stem increment (dW_s/dt) can now be expressed as:

$$204 \quad dW_s/dt = y A_c [P_0 (1 - \exp(-kL)) - \rho_s (1 - f_c/2) H r_s/c - L \zeta r_r] \\
 205 \quad - L (\pi c/4a) [aD (1 - H/H_m) + H] (1/\sigma + \zeta) dD/dt - L A_c (1/\sigma \tau_f + \zeta/\tau_r) \quad (16)$$

206 The annual increment in (dD/dt) and all the other diameter-related indices are simulated by combining Eq. (7)
 207 and Eq. (16).

208 2.1.3 Definition of the growing season

209 The season over which GPP is accumulated (i.e. the effective growing season) is defined as running from July
 210 in the previous year through to the end of June in the current year. This definition is consistent with the fact
 211 that photosynthesis peaks around the time of the summer solstice (Bauerle et al., 2012) and that maximum leaf
 212 area occurs shortly after this (Rautiainen et al., 2012). Carbon fixed during the later half of the year (July to
 213 December) is therefore either stored or allocated to purposes other than foliage expansion. Observations of
 214 tree radial growth show that it can occur before leaf-out (in broadleaved trees) or leaf expansion (in
 215 needleleaved trees), thus confirming that some part of this growth is based on starch reserves from the
 216 previous year (Michelot et al., 2012). This definition of the effective growing season is also supported by
 217 analyses of our data which showed that correlations between simulated and observed tree ring-widths are
 218 poorer when the model is driven by GPP during the current calendar year rather than an effective growing
 219 season from July through June.

220 2.2 Model application

221 2.2.1 Observations

222 We use site-specific information on climate and tree growth from a relatively low-elevation site (ca 128°02'E,
223 42°20'E, 800 m a.s.l.) in mixed conifer and broadleaf virgin forest in the Changbai Mountains, northeastern
224 China (Bai et al., 2008). This region was chosen because there is no evidence of human influence on the
225 vegetation, and the forests are maintained by natural regeneration. Data on tree height, diameter and crown
226 area were collected for 400 individual *Pinus koraiensis* trees from thirty-five 20m by 20m sample plots. The
227 400 trees included all individual of this species in the 35 plots, i.e. represent a complete sampling of the
228 variability in growth. Tree height and diameter were measured directly, and crown area measured as the area
229 of projected ground coverage. Tree-ring cores were obtained from 46 of these individuals in 2007. The
230 selected trees were either from the canopy layer or from natural gaps in the forest, and in both cases not
231 overshadowed by nearby individuals in order to minimize the possible effects of competition. An attempt was
232 made to select individuals of different diameters (diameter at breast height from 10 to 70 cm at time of
233 sampling), broadly corresponding to the range of diameters recorded in the original sampling. The 46 trees
234 were of different ages (ranging from < 50 to ca. 200 years at the time of sampling, 2006); subsequent analyses
235 show there is little relationship between age and diameter at breast height. Environmental conditions (e.g. soil
236 depth, light availability) were relatively uniform across the sampling plot. Monthly temperature, precipitation
237 and fractional cloud cover data, from 1958 onwards, were obtained from Songjiang meteorological station
238 (128°15'E, 42°32'E, 591.4 m a.s.l.), which is representative of the regional climate at low elevations in the
239 Changbai Mountains.

240 2.2.2 Derivation of T model parameter values

241 T model parameter values were derived from measurements made at the sampling site or from the literature
242 (Table 1). We estimated the initial slope of the height-diameter relationship (a : 116), the initial ratio of crown
243 area to stem cross-sectional area (c : 390.43), and maximum tree height (H_m : 25.33 m) using nonlinear
244 regression applied to diameter at breast height (D), tree height (H), and crown area (A_c) measurement on all
245 the 400 trees from the sample plots (Fig. 2). We used a value of sapwood density derived from three
246 measurements at the sampling site (Table 1). We used values of leaf area index within the crown (L), specific
247 leaf area (σ), foliage turnover time (τ_f), and fine-root turnover time (τ_r) for *Pinus koriensis* from field studies
248 conducted in northeastern China (Table 1). No species-specific information was available for the PAR
249 extinction coefficient (k), yield factor (y), ratio of fine-root mass to foliage area (ζ), fine-root specific
250 respiration rate (r_r), or sapwood specific respiration rate (r_s). We therefore used published values for other
251 species of evergreen needleleaf trees, taken from papers that summarise results from a range of field
252 measurements. Most of the published values for these parameters fall in a relatively narrow range (Table 1).
253 The uncertainty in fine-root specific respiration rate is not given in the original source paper (Yan and Zhao,
254 2007) but the average value is consistent with other studies (e.g. Zogg et al., 1996). The published values for

255 sapwood-specific respiration rate in pines show considerable variability, ranging from 0.5~10, or even 20
256 nmol/mol/s (Landsberg and Sands, 2010). Analyses (see Sect. 3.1) show that the model is sensitive to the
257 specification of sapwood respiration. We therefore selected the final value for this parameter based on
258 calibration of the simulated mean ring width against observations, constrained by the published range of
259 values for sapwood respiration rate.

260 2.3 Model application

261 We applied the model to simulate the growth of 46 individual *Pinus koraiensis* trees from the study site
262 between 1958-2006. The 46 trees were of different ages (ranging from <50 to ca 200 years at the time of
263 sampling, 2006) and different diameters (diameter at breast height from 10 to 70 cm at time of sampling).
264 Environmental conditions (e.g. soil depth, light availability) were relatively uniform across the sampling plot.
265 The start date for the simulations was determined by the availability of local climate data. Site latitude,
266 elevation, and observed monthly temperature, precipitation, fraction of cloud cover were used as input for the
267 P model. Each tree was initialised at its actual diameter at 1958, calculated from the measured diameter in
268 2007 and measured radial growth between 1958 and 2007. The model was initially run with a fixed CO₂
269 concentration of 360ppm. To examine the impact of changing atmospheric CO₂ levels on tree growth, we
270 made a second simulation using the observed monthly CO₂ concentration between 1958 and 2006 (310 - 390
271 ppm: NOAA ESRL).

272 2.4 Statistical methods

273 For statistical analyses and comparison with observations, the individual trees were grouped into three
274 cohorts, based on their age in 1958: young (0-49 years), mature (50-99 years), and old (>100 years).
275 Individual trees within each cohort exhibit a range of diameters: young ca 20-37 cm, mature: 9-59 cm, and
276 old: 25-40 cm. These differences in size will affect the expression of ontogeny within each cohort. The mean
277 and standard deviation (SD) of year-by-year diameter growth was calculated for each age cohort from the
278 observations and the simulations. The Pearson correlation coefficient and root mean squared error (RMSE)
279 were used to evaluate the degree of agreement between the observations and simulations. We used generalised
280 linear modelling (GLM: McCullagh, 1984) to analyse the response of tree growth to the major climate factors
281 and age. The GLM approach is helpful for separating the independent influence of individual factors on tree
282 growth, given the inevitable existence of correlations between these factors.

283

284 3 Results

285 3.1 Simulated ring width versus observation

286 There are only small differences between different age cohorts in the mean simulated ring width, with a mean
287 value of 1.43 mm for young trees, 1.31 mm for mature trees, and 1.37 for older trees. These values are

288 comparable to the mean value obtained from the observations (1.48mm, 1.29mm, 1.34mm respectively).
289 However, the general impact of ageing is evident in the decreasing trend in ring widths between 1958 and
290 2007 within any one cohort (Fig. 3). The slope is stronger in the observations than in the simulations,
291 indicating that the model somewhat underestimates the effects of ontogeny.

292 There is considerable year-to-year variability in tree growth. The simulated interannual variability (standard
293 deviation) in simulated ring width is similar in all the age cohorts (0.265 mm in the young, 0.265 mm in the
294 mature, and 0.264 mm in the old trees). This variability is somewhat less than shown by the observations,
295 where interannual variability is 0.274mm, 0.367mm, 0.245mm respectively in the young, mature and old
296 cohorts. The RMSE is 0.263mm, 0.332mm, and 0.284mm respectively for young, mature and old age cohorts.
297 The correlation between the observed and simulated sequence in each cohort is statistically significant ($P =$
298 0.000, 0.001, 0.009 respectively for young, mature and old age cohorts).

299 Despite the fact that the model reproduces both the mean ring width and the interannual variability in tree
300 growth reasonably well, the range of ring widths simulated for individual trees within any one cohort is much
301 less than the range seen in the observations. This is to be expected, given that individual tree growth is
302 affected by local factors (e.g. spatial variability in soil moisture) and may also be influenced by ecosystem
303 dynamics (e.g. opening up of the canopy through the death of adjacent trees) – effects that are not taken into
304 account in the model.

305 3.2 Parameter sensitivity analysis

306 To evaluate the sensitivity of the model to specification of individual parameters, we ran a series of
307 simulations in which individual parameter values were increased or decreased by 50% of their reference
308 value. For each of these simulations, the T model was run for 500 years using constant potential GPP (the
309 mean GPP during the period 1958-2006).

310 The model simulates a rapid initial increase in ring width, with peak ring widths occurring after ca 10 years,
311 followed by a gradual and continuous decrease with age (Fig. 4). The model is comparatively insensitive to
312 uncertainties in the specification of fine-root specific respiration rate (r_r), fine-root turnover time (τ_f), and
313 specific leaf area (σ), while leaf area index within the crown (L), ratio of fine-root mass to foliage area (ζ) and
314 fine-root turnover time (τ_r) have only a moderate effect on the simulated amplitude of ring width. The largest
315 impacts on the amplitude of the simulated ring width are from initial slope of height-diameter relationship (a),
316 initial ratio of crown area to stem cross-sectional area (c), and sapwood density (ρ_s). Maximum tree height
317 (H_m) and sapwood-specific respiration rate (r_s) have the greatest influence on the shape of the simulated
318 ageing curve. These two parameters also have a large impact on the amplitude of the growth of old trees. The
319 parameters values for a , c , H_m and ρ_s are derived from observations, with uncertainties much less than 50%
320 (Fig. 2). Thus, the sensitivity of the model to these parameters is not important. However, model sensitivity to
321 sapwood respiration (r_s) both in terms of the shape of the ageing curve and the amplitude is of greater

322 concern, given the large range of values in the literature. Although some part of the uncertainty in the
323 specification of sapwood respiration may be due to differences between species, the difficulty of measuring
324 this trait accurately also contributes to the problem. For the final model, we tuned r_s against the ring-width
325 observations. The best match with the observations was obtained with a value 1.4 nmol/mol/s, which is within
326 the range of published values for pines (see summary in Landsberg and Sands, 2010). r_s is the only parameter
327 that was tuned.

328 3.3 Controls on tree growth

329 The GLM analysis revealed a strong positive relationship between PAR_0 and tree growth, while moisture
330 stress (as measured by α , an estimate of the ratio of actual to potential evapotranspiration) was shown to have
331 a less steep but still positive effect (Fig. 5 and Table 2). The observed partial relationship between mean
332 annual temperature and tree growth is negative. The Changbai Mountains are at the southern end of the
333 distribution of *Pinus koraiensis* in China, which makes it plausible that tree growth would be inhibited during
334 warmer years.

335 The model reproduces these observed relationships between climate factors and tree growth. The slope of the
336 observed positive relationship with α is statistically indistinguishable from the modelled slope, but the
337 observed positive relationship with PAR_0 is weaker, and the negative correlation with mean annual
338 temperature is stronger, in the observations than in the simulations. These differences between observations
339 and simulations could reflect the influence of an additional climate control, related to both PAR_0 and
340 temperature (e.g. cloud cover). The difference between observed and simulated effects of temperature may
341 also be because although simulated growth is inhibited by low temperatures (through the computation of
342 PAR_0), the current model does not include any mechanism for inhibition due to heat stress at high air and leaf
343 temperatures.

344 The GLM analysis also showed that age, as represented by the three age cohorts, has an impact on ring width:
345 young trees have greater ring widths than mature trees, while old trees have somewhat greater ring widths
346 than mature trees. This pattern is seen in both the observations and simulations, although the differences
347 between the young and mature cohorts are slightly greater in the observations.

348 The overall similarity in the observed and simulated relationships between growth rates and environmental
349 factors confirms that the T model performs realistically. The observed relationships are considerably noisier
350 than the simulated relationships (Fig. 5, Table 2), reflecting the fact that growth rates are affected by small-
351 scale variability in environmental conditions as well as time-varying competition for light.

352 3.4 Simulated CO₂ effect on tree growth

353 Elevated levels of CO₂ are expected to have a positive impact on tree growth (Hyvönen et al., 2007; Donohue
354 et al., 2013; Hickler et al., 2008; Boucher et al., 2014). This positive response to [CO₂] is seen in the

355 comparison of the fixed [CO₂] and real [CO₂] simulations (Fig. 5). In the first part of the simulation, prior to
356 1980, the actual [CO₂] is lower than the level of 360 ppm used in the fixed [CO₂] experiment: this results in
357 lower growth rates. The 50 ppm difference between the two experiments at the beginning of the simulation
358 results in a difference in ring width of 0.242 mm. After 1980, when the actual [CO₂] was higher than 360
359 ppm, the tree growth in the simulation with realistic [CO₂] is enhanced. The 30 ppm difference at the end of
360 the simulation results in a difference in ring width of 0.101 mm. Overall, the change in [CO₂] between 1958
361 and 2006 results in a positive enhancement of tree growth of ca 0.343 mm/yr. However, this difference is very
362 small compared to the impact of ageing (> 1 mm from observations) or to the differences resulting from the
363 interannual variability of climate (1.212 mm) on tree growth.

364

365 4 Discussion

366 We have shown that radial growth (ring width) can be realistically simulated by coupling a simple generic
367 model of GPP with a model of carbon allocation and functional geometric tree growth with species-specific
368 values. The model is responsive to changes in climate variables, and can account for the impact of changing
369 CO₂ and ontogeny on tree growth. Although several models draw on basic physiological and/or geometric
370 constraints in order to simulate tree-ring indices (Fritts, 2012; Vaganov et al., 2006; Rathgeber et al., 2005;
371 Misson, 2004), and indeed the two approaches have been combined to simulate between-site differences in
372 ecosystem productivity and tree growth (Härkönen et al. 2010; Härkönen et al. 2013), this is the first time to
373 our knowledge that the two approaches have been combined to yield an explicit treatment of individual tree-
374 growth processes, tested against an extensive ring-width data set.

375 Our simulations suggest that after a brief but rapid increase for young plants, there is a general and continuous
376 decrease in radial growth with age (Fig. 4). This pattern is apparent in individual tree-ring series, and is
377 evident in the decreasing trend in ring widths shown when the series are grouped into age cohorts (Fig. 3). It is
378 a necessary consequence of the geometric relationship between the stem diameter increment and cross-
379 sectional area: more biomass is required to produce the same increase in diameter in thicker, taller trees than
380 thinner, shorter ones. However, we find that ring widths in old trees in our study region are consistently wider
381 than in mature trees, and this property is reproduced in the simulations (Fig. 5). This situation arises because
382 the old trees are on average smaller than the mature trees at the start of the simulation (in 1958). Thus, while
383 the difference between average ring-widths in the mature and old cohorts conforms to the geometric
384 relationship between stem diameter increment and cross-sectional area, it is a response that also reflects
385 differences in the history of tree growth at this site which determined the initial size of the trees in 1958. Lack
386 of climate data prior to 1958 or detailed information about stand dynamics precludes diagnosis of the cause of
387 the growth history differences between mature and old trees.

388 Studies attempting to isolate the impact of climate variability on tree growth, including attempts to reconstruct
389 historical climate changes using tree-ring series, often describe the impact of ageing as a negative exponential
390 curve (Fritts, 2012). However, our analyses suggest that this is not a good representation of the actual effect of
391 ageing on tree growth, and would result in masking of the impact of climate-induced variability in mature and
392 old trees. The simulated NPP of individual trees always increases with size (or age). This is consistent with
393 the observation that carbon sequestration increases continuously with individual tree size (Stephenson et al.,
394 2014).

395 We have shown that total PAR during the growing season is positively correlated with tree growth at this site.
396 This is not surprising given that PAR is the primary driver of photosynthetic carbon fixation. However, none
397 of the empirical or semi-empirical models of tree growth uses PAR directly as a predictor variable; most use
398 some measure of seasonal or annual temperature as a surrogate. PAR is determined by latitude and cloudiness.
399 Although temperature varies with latitude and cloudiness, it is also influenced by other factors including heat
400 advection. Temperature changes can impact the length of the growing season, and hence have an impact on
401 total growing-season PAR, but this is a trivial effect over recent decades. In fact, we show that mean annual
402 temperature *per se* is negatively correlated with tree growth at this site. Given this decoupling, and the
403 potential that longer-term changes in cloudiness will not necessarily be correlated with changes in temperature
404 (Charman et al., 2013), we strongly advocate the use of growing-season PAR for empirical modelling as well
405 as in process-based modelling.

406 We found no age-related sensitivity to inter-annual variability in climate: the interannual variability in ring
407 width is virtually identical between age cohorts. The strength of the relationship with individual climate
408 variables is also similar between the three age cohorts. It is generally assumed that juvenile and old trees are at
409 greater risk of mortality from environmental stress than mature trees (e.g. Lines et al., 2010; McDowell et al.,
410 2008). This may be true in the case of extreme events, such as wildfires or windthrow, or pest attack. Our
411 results suggest that although climate variability has an important effect on tree growth it is not an important
412 influence on mortality.

413 We have assumed that the period contributing to growth (i.e. the effective growing season) in any year
414 includes carbon stores generated during the second half of the previous year. The total foliage area determines
415 the radial area of the stem, and once this is achieved NPP is allocated either to fine root production or stored
416 as carbohydrate for use in stem growth in the early part of the subsequent year. This is consistent with
417 observations that radial growth begins before leaf-out (Michelot et al., 2012) and that maximum leaf area is
418 generally achieved by mid-summer (Rautiainen et al., 2012), and the MAIDEN model also allows tree growth
419 to be influenced by a fixed contribution from the previous year's growth (Misson, 2004). Defining the
420 effective growing season as being only the current growth year had no impact on the influence of climate on
421 ring widths, or the shape of the aging curve. It did, however, produce a considerably lower correlation
422 between simulated and observed inter-annual variability in growth. Since tree ring-width reflects the

423 integrated climate over the “effective growing season”, reconstructions of climate variables reflect conditions
424 during that season, not simply during the current calendar year.

425 The high degree of autocorrelation present in tree-ring series is often seen as a problem requiring pre-
426 treatment of the series in order to derive realistic reconstructions of climate variables (e.g. Cook et al., 2012;
427 Anchukaitis et al., 2013; Wiles et al., 2014). However, spatial or temporal autocorrelation is a reflection of the
428 causal mechanism underpinning the observed patterning. Here we postulate that the mechanism that gives rise
429 to the temporal autocorrelation in tree-ring series is the existence of carbon reserves that are created in one
430 year and fuel early growth in the next. If a large reserve of carbon is created in the second half of the growing
431 season, because of favourable conditions, this will offset poor conditions in the following year. However,
432 large reserves may not be necessary if conditions during the subsequent growing year are very favourable.
433 The fact that the relative influence of one year on the next can vary explains why the measured autocorrelation
434 strength in a given tree-ring series varies through time.

435 The T model is sensitive to the values adopted for some parameters, specifically the initial slope of height-
436 diameter relationship (a), the initial ratio of crown area to stem cross-sectional area (c), maximum tree height
437 (H_m), sapwood density (ρ_s), sapwood specific respiration rate (r_s), leaf area index within the crown (L), ratio of
438 fine-root mass to foliage area (ζ) and fine-root turnover time (τ_r). Several of these parameters are easily
439 derived from observations (e.g. a , c , H_m , ρ_s , L) and provided that sufficient site-based observations are
440 available should not pose a problem for applications of the model. However, the model is also sensitive to less
441 easily measured parameters, including sapwood respiration, root respiration and the ratio of fine roots to
442 leaves. Estimates of values for root respiration and root mass to foliage area in the literature do not show
443 substantial differences, and we therefore used an average value to parameterize our model. This approach
444 could be used for other applications. We parameterized fine-root turnover rates based on observations on
445 *Pinus koriensis* from Changbai. While this obviated the need for tuning in the current application, lack of data
446 on fine-root turnover rates in other regions (or for other species) could pose problems for future applications
447 of the model. The model is also highly sensitive to the parameter value used for sapwood respiration and the
448 range of reported values is large (Table 1). Because of this, we derived a value for sapwood respiration by
449 tuning the model to obtain a good representation of average ring width. This is the only parameter that
450 requires tuning in the current version of the T model. Although sapwood respiration is difficult to measure, it
451 would certainly be better if more measurements of sapwood respiration were available, as this would remove
452 the need for model tuning.

453 Our modelling approach integrates the influence of climate, [CO₂] and ontogeny on individual tree growth.
454 Such a model is useful to explore the response of tree growth to potential future changes in climate, and the
455 impact of changes in tree growth on carbon sequestration. We also envisage that it could also be used to
456 investigate the impact of past climate changes on tree growth. Reconstructions of temperature changes beyond
457 the recent observational period, used as a baseline for the detection of anthropogenic influences on the climate

458 system, are largely derived from statistical reconstructions based on tree-ring series (Jones et al., 1998; Esper
459 et al., 2002; Hegerl et al., 2006; Mann et al., 2008; Ahmed et al., 2013). However, as we show here,
460 temperature is neither the only, nor the most important, influence on tree growth. This may help to explain
461 why correlations between ring-widths and climate at individual sites appear to have broken down in recent
462 decades (the so-called divergence problem: D'Arrigo et al., 2008). The availability of a robust model to
463 investigate tree growth could help to provide better reconstructions of past climate changes (see e.g. Boucher
464 et al., 2014) as well as more plausible projections of the response of tree growth to continuing climate change
465 in the future.

466

467 Acknowledgements.

468 We thank Wang Han for assistance with the P model. GL is supported by International Postgraduate Research
469 Scholarship at Macquarie University. The work is a contribution to the AXA Chair programme on Biosphere
470 and Climate Impacts and the Imperial College initiative Grand Challenges in Ecosystems and the
471 Environment.

472

473

474 References

- 475 Ahmed, M., Anchukaitis, K. J., Asrat, A., Borgaonkar, H. P., Braida, M., Buckley, B. M., Büntgen, U., Chase, B.
476 M., Christie, D. A., and Cook, E. R.: Continental-scale temperature variability during the past two millennia, *Nat.*
477 *Geosci.*, 6, 339-346, doi:10.1038/NNGEO1797, 2013.
- 478 Anchukaitis, K. J., D'Arrigo, R. D., Andreu-Hayles, L., Frank, D., Verstege, A., Curtis, A., Buckley, B. M.,
479 Jacoby, G. C., and Cook, E. R. Tree-Ring-Reconstructed Summer Temperatures from Northwestern North America
480 during the Last Nine Centuries. *J. Clim.*, 26, DOI: 10.1175/JCLI-D-11-00139.1, 3001-3012, 2013.
- 481 Bai, F., Sang, W., Li, G., Liu, R., Chen, L., and Wang, K.: Long-term protection effects of national reserve to forest
482 vegetation in 4 decades: biodiversity change analysis of major forest types in Changbai Mountain Nature Reserve,
483 China, *Sci. China Ser. C*, 51, 948-958, 2008.
- 484 Bauerle, W. L., Oren, R., Way, D. A., Qian, S. S., Stoy, P. C., Thornton, P. E., Bowden, J. D., Hoffman, F. M., and
485 Reynolds, R. F.: Photoperiodic regulation of the seasonal pattern of photosynthetic capacity and the implications
486 for carbon cycling, *P. Natl. Acad. Sci.*, 109, 8612-8617, doi:10.1073/pnas.1119131109, 2012.
- 487 Bernacchi, C., Pimentel, C., and Long, S.: In vivo temperature response functions of parameters required to model
488 RuBP-limited photosynthesis, *Plant Cell Environ.*, 26, 1419-1430, 2003.
- 489 Bonan, G. B.: Forests and climate change: forcings, feedbacks, and the climate benefits of forests, *Science*, 320,
490 1444-1449, doi:10.1126/science.1155121, 2008.
- 491 Boucher, É., Guiot, J., Hatté, C., Daux, V., Danis, P.-A., and Dussouillez, P.: An inverse modeling approach for
492 tree-ring-based climate reconstructions under changing atmospheric CO₂ concentrations, *Biogeosciences*, 11, 3245-
493 3258, doi:10.5194/bg-11-3245-2014, 2014.
- 494 Caspersen, J. P., Vanderwel, M. C., Cole, W. G., and Purves, D. W.: How stand productivity results from size-and
495 competition-dependent growth and mortality, *PLoS One*, 6, e28660, 2011.
- 496 Charman, D. J., Beilman, D.W., Blaauw, M., Booth, R.K., Brewer, S., Chambers, F.M., Christen, J.A. Gallego-Sala,
497 A., Harrison, S.P., Hughes, P.D.M., Jackson, S.T., Korhola, A., Mauquoy, D., Mitchell, F.J.G., Prentice, I.C., van
498 der Linden, M., de Vleeschouwer, F., Yu, Z.C., Alm, J., Bauer, I.E., Corish, Y.M.C., Garneau, M., Hohl, V., Huang,
499 Y., Karofeld, E., Le Roux, G., Moschen, R., Nichols, J.E., Nieminen, T., McDonald, G.M., Phadtare, N.R., Rausch,
500 N., Shotyk, W., Sillasoo, U., Swindles, G.T., Tuittila, E.S., Ukonmaanaho, L., Väliranta, M., van Bellen, S., van
501 Geel, B., Vitt, D.H., Zhao, Y.: Climate-driven changes in peatland carbon accumulation during the last millennium,
502 *Biogeosciences*, 10, 929-944, doi:10.5194/bg-10-929-2013, 2013.
- 503 Chen, G., DAI, L., and ZHOU, L.: Structure of stand and canopy characteristics of disturbed communities of
504 broadleaved *Pinus koraiensis* forest in Changbai Mountain [J], *Chin. J. Ecol.*, 23, 116-120, 2004.
- 505 Ciais, P., Sabine, C., Bala, G., Bopp, L., Brovkin, V., Canadell, J., Chhabra, A., DeFries, R., Galloway, J., Heimann,
506 M., Jones, C., Quéré, C. L., Myneni, R. B., Piao, S., and Thornton, P.: Carbon and Other Biogeochemical Cycles.
507 In: *Climate Change 2013: The Physical Science Basis. Contribution of Working Group I to the Fifth Assessment*
508 *Report of the Intergovernmental Panel on Climate Change*. [Stocker, T.F., D. Qin, G.-K. Plattner, M. Tignor, S.K.
509 Allen, J. Boschung, A. Nauels, Y. Xia, V. Bex and P.M. Midgley (eds.)], Cambridge University Press, Cambridge,
510 UK and New York, NY, USA, 2013.
- 511 Claesson, J., and Nycander, J.: Combined effect of global warming and increased CO₂-concentration on vegetation

512 growth in water-limited conditions, *Ecol. Model.*, 256, 23-30, 2013.

513 Cook, E. R., Krusic, P. J., Anchukaitis, K. J., Buckley, B. M., Nakatsuka, T., & Sano, M.: Tree-ring reconstructed
514 summer temperature anomalies for temperate East Asia since 800 CE. *Clim. Dyn.*, 41(11-12), 2957-2972, DOI
515 10.1007/s00382-012-1611-x, 2012.

516 Cruiziat, P., Cochard, H., and Améglio, T.: Hydraulic architecture of trees: main concepts and results, *Ann. For.*
517 *Sci.*, 59, 723-752, doi: 10.1051/forest:2002060, 2002.

518 D'Arrigo, R., Wilson, R., Liepert, B., and Cherubini, P.: On the 'divergence problem' in northern forests: a review
519 of the tree-ring evidence and possible causes, *Global Planet. Change*, 60, 289-305, 2008.

520 Danis, P.-A., Hatté, C., Misson, L., and Guiot, J.: MAIDENiso: a multiproxy biophysical model of tree-ring width
521 and oxygen and carbon isotopes, *Can. J. Forest Res.*, 42, 1697-1713, 2012.

522 Donohue, R. J., Roderick, M. L., McVicar, T. R., and Farquhar, G. D.: Impact of CO₂ fertilization on maximum
523 foliage cover across the globe's warm, arid environments, *Geophys. Res. Lett.*, 40, 3031-3035,
524 doi:10.1002/grl.50563, 2013.

525 Duursma, R. A., Mäkelä, A., Reid, D. E., Jokela, E. J., Porté, A. J., and Roberts, S. D.: Self-shading affects
526 allometric scaling in trees, *Funct. Ecol.*, 24, 723-730, doi:10.1111/j.1365-2435.2010.01690.x, 2010.

527 Esper, J., Cook, E. R., and Schweingruber, F. H.: Low-frequency signals in long tree-ring chronologies for
528 reconstructing past temperature variability, *Science*, 295, 2250-2253, doi:10.1126/science.1066208, 2002.

529 Falster, D. S., and Westoby, M.: Tradeoffs between height growth rate, stem persistence and maximum height
530 among plant species in a post-fire succession, *Oikos*, 111, 57-66, 2005.

531 Falster, D. S., Brännström, Å., Dieckmann, U., and Westoby, M.: Influence of four major plant traits on average
532 height, leaf-area cover, net primary productivity, and biomass density in single-species forests: a theoretical
533 investigation, *J. Ecol.*, 99, 148-164, doi:10.1111/j.1365-2745.2010.01735.x, 2011.

534 Friedlingstein, P., and Prentice, I.: Carbon-climate feedbacks: a review of model and observation based estimates,
535 *Curr. Opin. Environ. Sustainability*, 2, 251-257, 2010.

536 Fritts, H. C.: *Tree rings and climate*, Academic Press, London, 2012.

537 Gallego-Sala, A.V., Clark, J.M., House, J.I., Orr, H.G., Prentice, I.P., Smith, P. et al: Bioclimatic envelope model
538 of climate change impacts on blanket peatland distribution in Great Britain, *Clim Res* 45:151–162, 2010.

539 Givnish, T. J.: Adaptation to sun and shade: a whole-plant perspective, *Funct. Plant Biol.*, 15, 63-92,
540 doi:10.1071/PP9880063 1988.

541 Härkönen, S., Pulkkinen, M., Duursma, R., and Mäkelä, A.: Estimating annual GPP, NPP and stem growth in
542 Finland using summary models, *Forest. Ecol. Manag.*, 259, 524-533, 2010

543 Härkönen, S., Tokola, T., Packalén, P., Korhonen, L., and Mäkelä, A.: Predicting forest growth based on airborne
544 light detection and ranging data, climate data, and a simplified process-based model, *Can. J. For. Res.*, 43, 364-375,
545 2013.

546 Harrison, S. P., Prentice, I. C., Barboni, D., Kohfeld, K. E., Ni, J., and Sutra, J. P.: Ecophysiological and bioclimatic
547 foundations for a global plant functional classification, *J. Veg. Sci.*, 21, 300-317, doi:10.1111/j.1654-
548 1103.2009.01144.x, 2010.

549 Hegerl, G. C., Crowley, T. J., Hyde, W. T., and Frame, D. J.: Climate sensitivity constrained by temperature
550 reconstructions over the past seven centuries, *Nature*, 440, 1029-1032, doi:10.1038/nature04679, 2006.

551 Hickler, T., Smith, B., Prentice, I. C., Mjöfors, K., Miller, P., Arneth, A., and Sykes, M. T.: CO₂ fertilization in

552 temperate FACE experiments not representative of boreal and tropical forests, *Global Change Biol.*, 14, 1531-1542,
553 doi:10.1111/j.1365-2486.2008.01598.x, 2008.

554 Huang, J., Bergeron, Y., Denneler, B., Berninger, F., and Tardif, J.: Response of forest trees to increased
555 atmospheric CO₂, *Crit. Rev. Plant Sci.*, 26, 265-283, doi:10.1080/07352680701626978, 2007.

556 Huo, H., and Wang, C.: Effects of canopy position and leaf age on photosynthesis and transpiration of *Pinus*
557 *koraiensis*, *Chin. J. Appl. Ecol.*, 18, 1181-1186, 2007.

558 Hyvönen, R., Ågren, G. I., Linder, S., Persson, T., Cotrufo, M. F., Ekblad, A., Freeman, M., Grelle, A., Janssens, I.
559 A., and Jarvis, P. G.: The likely impact of elevated [CO₂], nitrogen deposition, increased temperature and
560 management on carbon sequestration in temperate and boreal forest ecosystems: a literature review, *New Phytol.*,
561 173, 463-480, doi:10.1111/j.1469-8137.2007.01967.x, 2007.

562 Ishii, H., Reynolds, J. H., Ford, E. D., and Shaw, D. C.: Height growth and vertical development of an old-growth
563 *Pseudotsuga-Tsuga* forest in southwestern Washington State, USA, *Can. J. Forest Res.*, 30, 17-24, 2000.

564 Jarvis, P. G., and Leverenz, J. W.: Productivity of temperate, deciduous and evergreen forests, in: *Physiological*
565 *plant ecology IV*, Springer, Berlin Heidelberg, 233-280, 1983.

566 Jones, P. D., Briffa, K. R., Barnett, T. P., and Tett, S. F. B.: High-resolution palaeoclimatic records for the last
567 millennium: interpretation, integration and comparison with General Circulation Model control-run temperatures,
568 *Holocene*, 8, 455-471, doi:10.1191/095968398667194956, 1998.

569 Jonson, T.: Taxatoriska undersökningar om skogsträdens form: (1) granens stamform. *Skogsvårdför, Tidskrift*, 8,
570 285-328, 1910.

571 King, D. A.: Size-related changes in tree proportions and their potential influence on the course of height growth,
572 in: *Size-and age-related changes in tree structure and function*, Springer, Netherlands, 165-191, 2011.

573 Körner, C.: Plant CO₂ responses: an issue of definition, time and resource supply, *New Phytol.*, 172, 393-411, 2006.

574 Koutavas, A.: CO₂ fertilization and enhanced drought resistance in Greek firs from Cephalonia Island, Greece,
575 *Global Change Biol.*, 19, 529-539, doi:10.1111/gcb.12053, 2013.

576 Landsberg, J. J., and Sands, P.: *Physiological ecology of forest production: principles, processes and models*,
577 Academic Press, 2010.

578 Larson, P. R.: Stem form development of forest trees, *For. Sci., Monograph 5*, 1-42, 1963.

579 Lines, E. R., Coomes, D. A., and Purves, D. W.: Influences of forest structure, climate and species composition on
580 tree mortality across the eastern US, *PLoS One*, 5, e13212, doi:10.1371/journal.pone.0013212, 2010.

581 Lloyd, J.: The CO₂ dependence of photosynthesis, plant growth responses to elevated CO₂ concentrations and their
582 interaction with soil nutrient status, II. Temperate and boreal forest productivity and the combined effects of
583 increasing CO₂ concentrations and increased nitrogen deposition at a global scale, *Funct. Ecol.*, 13, 439-459, 1999.

584 Luo, T.: Patterns of net primary productivity for Chinese major forest types and their mathematical models, Doctor
585 of Philosophy, Chinese Academy of Sciences, Beijing, 1996.

586 Luo, Y., Su, B., Currie, W. S., Dukes, J. S., Finzi, A., Hartwig, U., Hungate, B., McMurtrie, R. E., Oren, R., and
587 Parton, W. J.: Progressive nitrogen limitation of ecosystem responses to rising atmospheric carbon dioxide,
588 *Bioscience*, 54, 731-739, 2004.

589 Mäkelä, A., Landsberg, J., Ek, A. R., Burk, T. E., Ter-Mikaelian, M., Ågren, G. I., Oliver, C. D., and Puttonen, P.:
590 Process-based models for forest ecosystem management: current state of the art and challenges for practical
591 implementation, *Tree physiol.*, 20, 289-298, 2000.

592 Mann, M. E., Zhang, Z., Hughes, M. K., Bradley, R. S., Miller, S. K., Rutherford, S., and Ni, F.: Proxy-based
593 reconstructions of hemispheric and global surface temperature variations over the past two millennia, *P. Natl. Acad.*
594 *Sci. USA*, 105, 13252-13257, doi:10.1073/pnas.0805721105, 2008.

595 McCullagh, P.: Generalized linear models, *Eur. J. Oper. Res.*, 16, 285-292, 1984.

596 McDowell, N., Pockman, W. T., Allen, C. D., Breshears, D. D., Cobb, N., Kolb, T., Plaut, J., Sperry, J., West, A.,
597 and Williams, D. G.: Mechanisms of plant survival and mortality during drought: why do some plants survive while
598 others succumb to drought?, *New Phytol.*, 178, 719-739, doi:10.1111/j.1469-8137.2008.02436.x, 2008.

599 Medvigy, D., and Moorcroft, P. R.: Predicting ecosystem dynamics at regional scales: an evaluation of a terrestrial
600 biosphere model for the forests of northeastern North America, *Philos. T. Roy. Soc. B.*, 367, 222-235, 2012.

601 Michelot, A., Simard, S., Rathgeber, C., Dufrêne, E., and Damesin, C.: Comparing the intra-annual wood formation
602 of three European species (*Fagus sylvatica*, *Quercus petraea* and *Pinus sylvestris*) as related to leaf phenology and
603 non-structural carbohydrate dynamics, *Tree physiol.*, 32, 1033-1045, doi:10.1093/treephys/tps052, 2012.

604 Miller, H. G.: Carbon \times nutrient interactions - the limitations to productivity, *Tree physiol.*, 2, 373-385, 1986.

605 Misson, L.: MAIDEN: a model for analyzing ecosystem processes in dendroecology, *Can. J. Forest Res.*, 34, 874-
606 887, doi:10.1139/X03-252, 2004.

607 Misson, L., Rathgeber, C., & Guiot, J.: Dendroecological analysis of climatic effects on *Quercus petraea* and *Pinus*
608 *halepensis* radial growth using the process-based MAIDEN model. *Can. J. For. Res.* **34**: 888–898, doi:
609 10.1139/X03-253, 2004.

610 Moorcroft, P., Hurtt, G., and Pacala, S. W.: A method for scaling vegetation dynamics: the ecosystem demography
611 model (ED), *Ecol. Monogr.*, 71, 557-586, 2001.

612 Moritz, M. A., Hurteau, M. D., Suding, K. N., and D'Antonio, C. M.: Bounded ranges of variation as a framework
613 for future conservation and fire management, *Ann. N. Y. Acad. Sci.*, 1286, 92-107, doi:10.1111/nyas.12104, 2013.

614 Pan, Y., Birdsey, R. A., Fang, J., Houghton, R., Kauppi, P. E., Kurz, W. A., Phillips, O. L., Shvidenko, A., Lewis, S.
615 L., and Canadell, J. G.: A large and persistent carbon sink in the world's forests, *Science*, 333, 988-993,
616 doi:10.1126/science.1201609, 2011.

617 Pierce, L. L., and Running, S. W.: Rapid estimation of coniferous forest leaf area index using a portable integrating
618 radiometer, *Ecology*, 1762-1767, 1988.

619 Prentice, I. C., Dong, N., Gleason, S. M., Maire, V., and Wright, I. J.: Balancing the costs of carbon gain and water
620 transport: testing a new theoretical framework for plant functional ecology, *Ecol. Lett.*, 17, 82-91,
621 doi:10.1111/ele.12211, 2014.

622 Rathgeber, C. B., Misson, L., Nicault, A., and Guiot, J.: Bioclimatic model of tree radial growth: application to the
623 French Mediterranean Aleppo pine forests, *Trees*, 19, 162-176, doi:10.1007/s00468-004-0378-z, 2005.

624 Rautiainen, M., Heiskanen, J., and Korhonen, L.: Seasonal changes in canopy leaf area index and MODIS
625 vegetation products for a boreal forest site in central Finland, *Boreal Environ. Res.*, 17, 72-84, 2012.

626 Reich, P. B., Hobbie, S. E., Lee, T., Ellsworth, D. S., West, J. B., Tilman, D., Knops, J. M., Naeem, S., and Trost, J.:
627 Nitrogen limitation constrains sustainability of ecosystem response to CO₂, *Nature*, 440, 922-925,
628 doi:10.1038/nature04486, 2006.

629 Shan, J., Tao, D., Wang, M., and Zhao, S.: Fine roots turnover in a broad-leaved Korean pine forest of Changbai
630 mountain, *Chin. J. Appl. Ecol.*, 4, 241-245, 1993.

631 Shevliakova, E., Stouffer, R. J., Malyshev, S., Krasting, J. P., Hurtt, G. C., and Pacala, S. W.: Historical warming

632 reduced due to enhanced land carbon uptake, *P. Natl. Acad. Sci. USA*, 110, 16730-16735, 2013.

633 Shinozaki, K., Yoda, K., Hozumi, K., and Kira, T.: A quantitative analysis of plant form-the pipe model theory: I.
634 Basic analyses, *Jap. J. Ecol.*, 14, 97-105, 1964.

635 Smith, B., Prentice, I. C., and Sykes, M. T.: Representation of vegetation dynamics in the modelling of terrestrial
636 ecosystems: comparing two contrasting approaches within European climate space, *Global Ecol. Biogeogr.*, 10,
637 621-637, 2001.

638 Stephenson, N. L., Das, A. J., Condit, R., Russo, S. E., Baker, P. J., Beckman, N. G., Coomes, D. A., Lines, E. R.,
639 Morris, W. K., and Rüger, N.: Rate of tree carbon accumulation increases continuously with tree size, *Nature*,
640 doi:10.1038/nature12914, 2014.

641 Thomas, S. C.: Asymptotic height as a predictor of growth and allometric characteristics in Malaysian rain forest
642 trees, *Am. J. Bot.*, 83, 556-556, 1996.

643 Vaganov, E. A., Hughes, M. K., and Shashkin, A. V.: Introduction and factors influencing the seasonal growth of
644 trees, Springer, Berlin Heidelberg, 2006.

645 Wang, H., Prentice, I. C., and Davis, T. W.: Biophysical constraints on gross primary production by the terrestrial
646 biosphere, *Biogeosciences Discuss.*, 11, 3209-3240, doi:10.5194/bgd-11-3209-2014, 2014.

647 White, M. A., Thornton, P. E., Running, S. W., and Nemani, R. R.: Parameterization and sensitivity analysis of the
648 BIOME-BGC terrestrial ecosystem model: net primary production controls, *Earth Interact.*, 4, 1-85, 2000.

649 Wiles, G. C., D'Arrigo, R., Barclay, D., Wilson, R. S., Jarvis, S. K., Vargo, L., and Frank, D.: Surface air
650 temperature variability reconstructed with tree rings for the Gulf of Alaska over the past 1200 years. *The Holocene*,
651 24, 198-208, 2014.

652 Wright, I. J., Reich, P. B., and Westoby, M.: Least-cost input mixtures of water and nitrogen for photosynthesis,
653 *Am. Nat.*, 161, 98-111, 2003.

654 Wullschleger, S. D., Tschaplinski, T. J., and Norby, R. J.: Plant water relations at elevated CO₂ - implications for
655 water-limited environments, *Plant Cell Environ.*, 25, 319-331, 2002.

656 Yan, X., and Zhao, J.: Establishing and validating individual-based carbon budget model FORCCHN of forest
657 ecosystems in China, *Acta Ecol. Sin.*, 27, 2684-2694, 2007.

658 Yokozawa, M., and Hara, T.: Foliage profile, size structure and stem diameter-plant height relationship in crowded
659 plant populations, *Ann. Bot.-London*, 76, 271-285, 1995.

660 Zhang, Y., Xu, M., Chen, H., and Adams, J.: Global pattern of NPP to GPP ratio derived from MODIS data: effects
661 of ecosystem type, geographical location and climate, *Global Ecol. Biogeogr.*, 18, 280-290, doi:10.1111/j.1466-
662 8238.2008.00442.x, 2009.

663 Zogg, G.P., Zak, D.R., Burton, A.J. and Pregitzer, K.S.: Fine root respiration in northern hardwood forests in
664 relation to temperature and nitrogen availability. *Tree Physiol.*, 16, 719-725, 1996.

665

666

667 Table and Figure Captions

668 Table 1. Parameter description and the derivation of parameter values.

669 Table 2. GLM analysis of tree growth response to the climatic factors and age, based on simulations and
670 observations. The dependent variable is mean ring width series (1958 to 2006) for each age cohort (young,
671 mature, old). The independent variables are the growing-season total annual photosynthetically active
672 radiation (PAR), mean annual temperature (MAT), the ratio of actual to potential evapotranspiration (α), with
673 age-cohort treated as a factor.

674 Figure 1. Model application flow. We combined the simple light-use efficiency and photosynthesis model (P
675 model) with a carbon allocation and functional geometric tree growth model to simulate tree growth (e.g. ring
676 width). The inputs to the P model are latitude, elevation, $[\text{CO}_2]$, and monthly temperature, precipitation, and
677 fractional cloud cover. Potential gross primary productivity (GPP), output by the P model, drives the T model,
678 together species-specific parameter values.

679 Figure 2. Estimation of parameter values for the application of the T model. Diameter at breast height (D),
680 tree height (H), and crown area (A_c) of the 400 trees from the sample plots were used for the estimation of the
681 initial slope of height-diameter relationship (a), and (asymptotic) maximum tree height (H_m). Relationships
682 among crown area (A_c) diameter at breast height (D) and height (H) (Eq. 7) are used to estimate the initial
683 ratio of crown area to stem cross-sectional area (c).

684 Figure 3. Comparison between simulations and observations for the three age-cohorts (young: 0-49 year,
685 mature: 50-99 year, and old >100 year). Each tree was initialised at its actual diameter at 1958, calculated
686 from the measured diameter in 2007 and measured radial growth between 1958 and 2007. The black line is
687 the mean of observations within each age-cohort, and grey bars are the standard deviation (SD) of individuals
688 within each age-cohort. The blue line and bars are the mean and standard deviation from the simulations.

689 Figure 4. Parameter sensitivity analyses for the T model. A constant input of gross primary productivity (GPP)
690 (mean during 1958-2006) was used to drive the T model to simulate tree growth for 500 years following
691 establishment. The black line was obtained with the reference value of each parameter. The effects of an
692 increase (150% of reference value, blue line) and a decrease (50% of reference value, red line) are also shown.

693 Figure 5. Tree growth response to climate and tree age: partial residual plots based on the GLM analysis
694 (Table 2), obtained using the visreg package in R, are shown.

695 Figure 6 CO_2 effect on tree growth. Two runs, one with a fixed 360ppm $[\text{CO}_2]$ (blue line), the other with
696 observed monthly $[\text{CO}_2]$ (red line), are compared to show the simulated effect of $[\text{CO}_2]$ on tree growth during
697 1958~2006.

Table 1

Parameter	Code	Value	Uncertainty or Range of value from literature	Value source: Observation or Published literature
initial slope of height-diameter relationship (-)	a	116	± 4.35	Observation (fig. 2)
initial ratio of crown area to stem cross-sectional area (-)	c	390.43	± 11.84	Observation (fig. 2)
maximum tree height (m)	H_m	25.33	± 0.71	Observation (fig. 2)
sapwood density (kgC m^{-3})	ρ_s	200	± 25	Observation
leaf area index within the crown (-)	L	1.8	1.5~1.96	Chen et al., 2004
specific leaf area ($\text{m}^2 \text{kg}^{-1} \text{C}$)	σ	14	13.22~16.82	Huo and Wang, 2007
foliage turnover time (year)	τ_f	4	-	Luo, 1996
fine-root turnover time (year)	τ_r	1.04	-	Shan et al., 1993
PAR extinction coefficient (-)	k	0.5	0.48-0.58	Pierce and Running, 1988
yield factor (-)	y	0.6	0.5~0.7	Zhang et al., 2009
ratio of fine-root mass to foliage area (kgC m^{-2})	ζ	0.17	± 0.198	White et al., 2000
fine-root specific respiration rate (year^{-1})	r_r	0.913	-	Yan and Zhao, 2007
sapwood specific respiration rate (year^{-1})	r_s	0.044 (1.4 nmol/mol/s)	0.5~10 (20) nmol/mol/s	Landsberg and Sands, 2010

Table 2

		Intercept (mm)	PAR (mm/kmol photon m ⁻²)	MAT (mm/°C)	α (mm)
	Estimation	-3.123	0.625	-0.180	0.702
Observation	Error	± 0.784	± 0.093	± 0.042	± 0.301
	p value	0.004	0.000	0.000	0.021
	Estimation	-7.139	1.056	-0.078	1.142
Simulation	Error	± 0.169	± 0.020	± 0.009	± 0.065
	p value	0.000	0.000	0.000	0.000

Figure 1

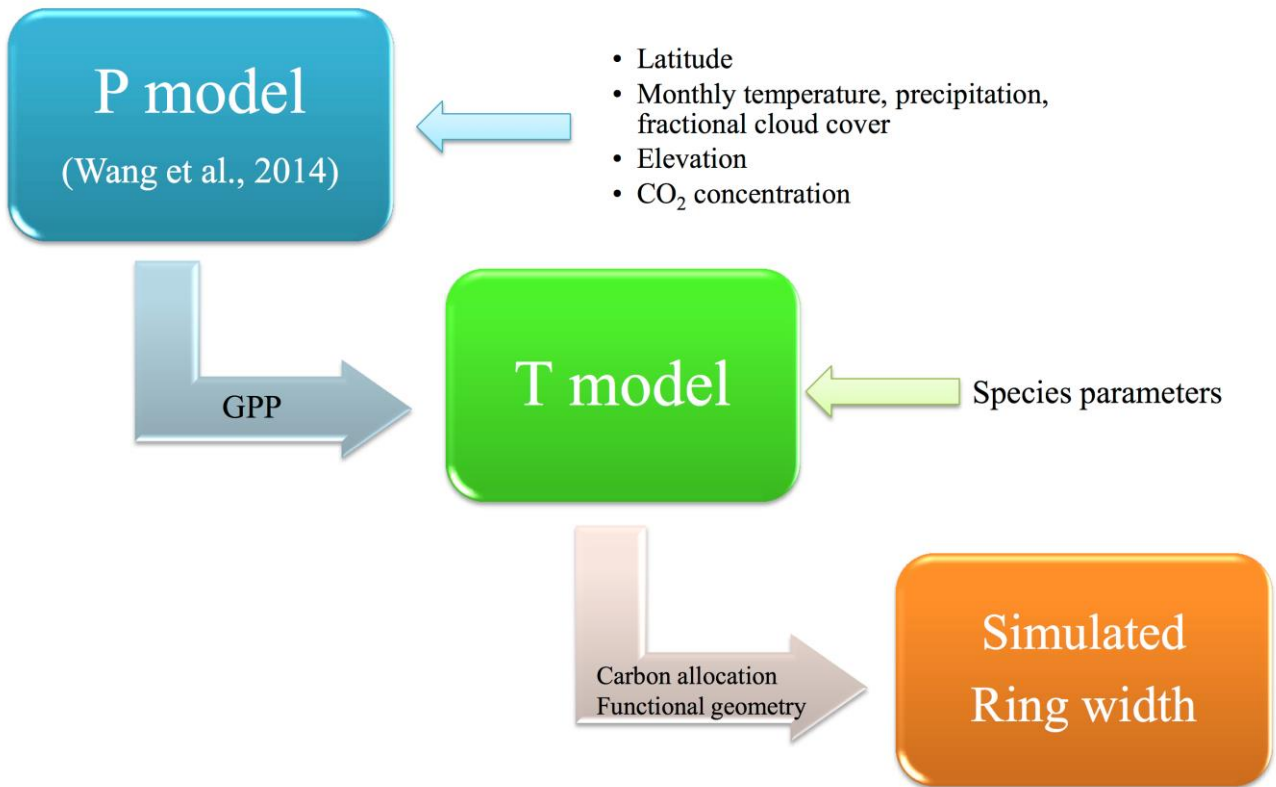


Figure 2

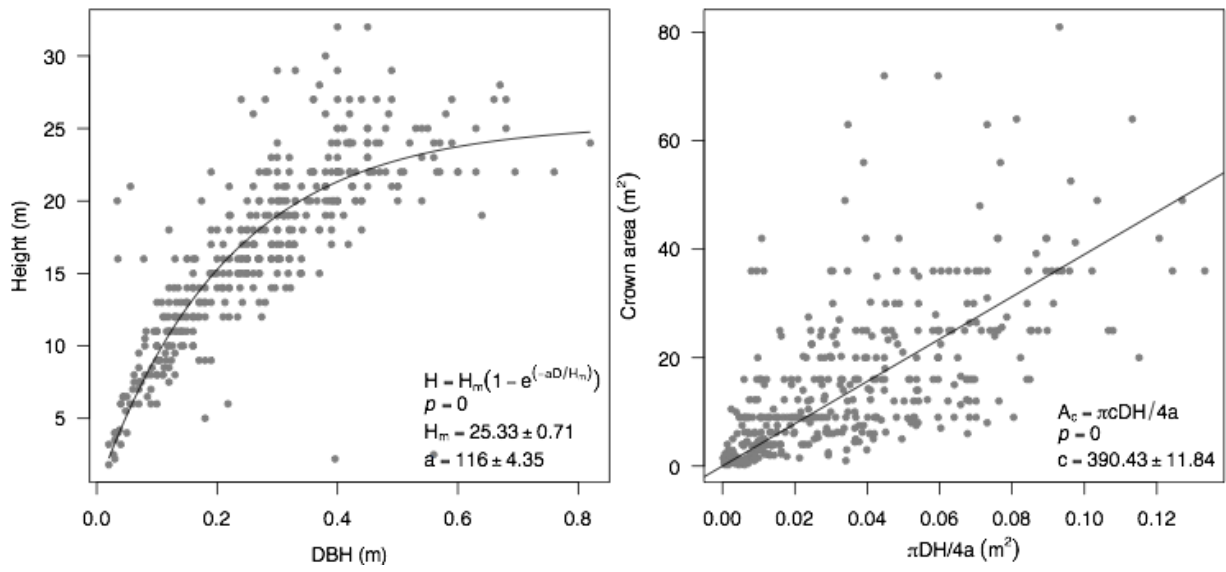


Figure 3

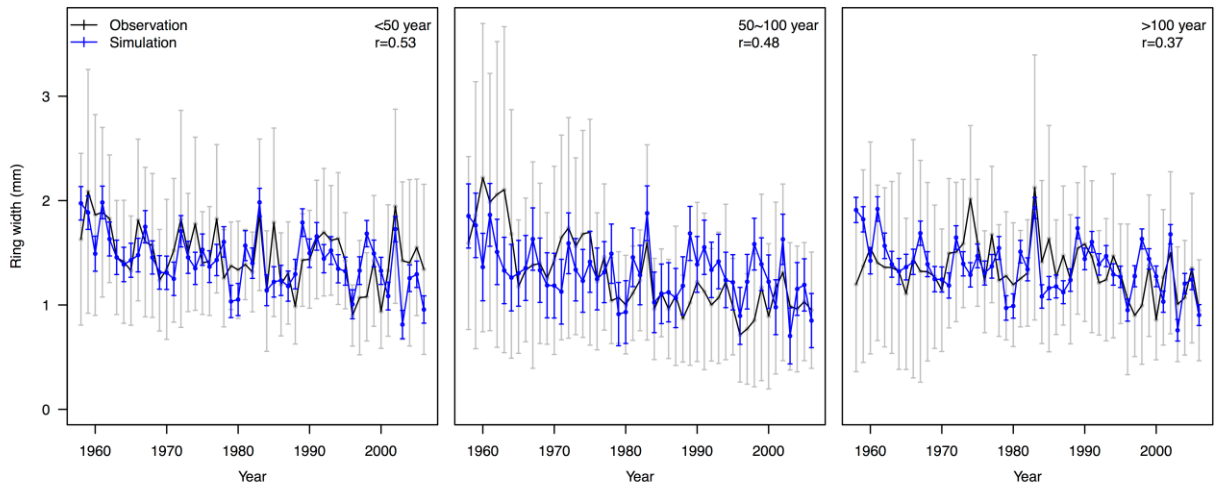


Figure 4

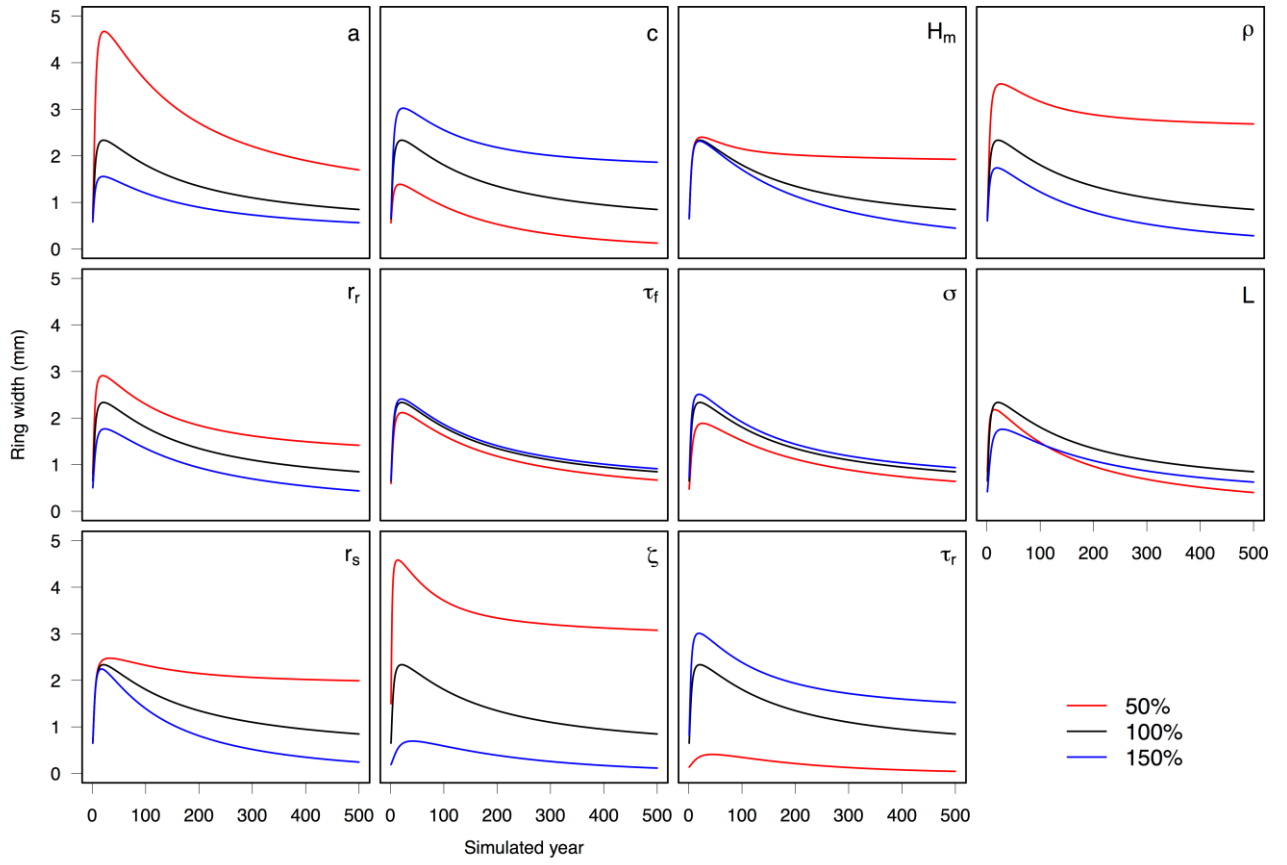


Figure 5

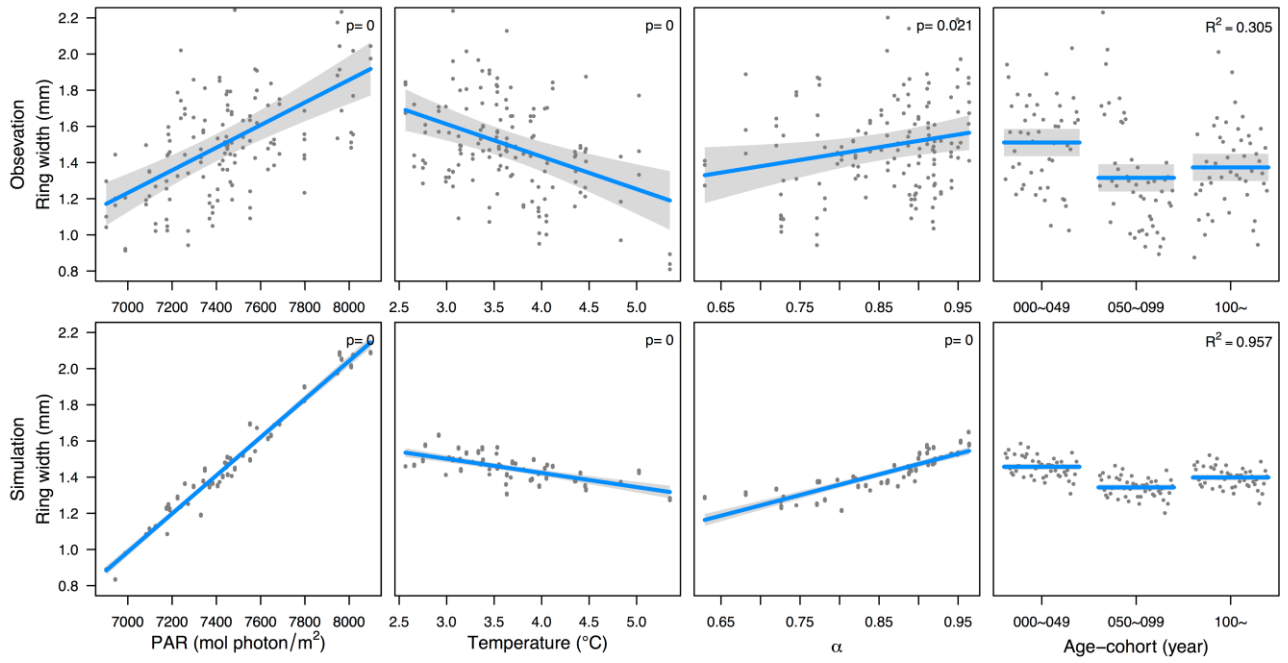


Figure 6

